



# An ultra-sensitive aptasensor on optical fibre for the direct detection of bisphenol A

Thomas D.P. Allsop<sup>a,c</sup>, Ronald Neal<sup>b</sup>, Changle Wang<sup>c,\*</sup>, David A. Nagel<sup>d</sup>, Anna V. Hine<sup>d</sup>, Philip Culverhouse<sup>b</sup>, Juan D. Ania Castañón<sup>a</sup>, David J. Webb<sup>c</sup>, Simona Scarano<sup>e</sup>, Maria Minunni<sup>e</sup>

<sup>a</sup> Non-linear Dynamics and Fiber Optics, Instituto de Óptica "Daza de Valdés" (IO-CSIC), Calle de Serrano, 121, 28006 Madrid, Spain

<sup>b</sup> Dept of Maths and Computing, Faculty of Science and Technology, University of Plymouth, Plymouth PL4 8AA, UK

<sup>c</sup> Aston Institute of Photonic Technologies, Aston University, Aston Triangle, Birmingham B47ET, UK

<sup>d</sup> School of Life and Health Sciences, Aston University, Aston Triangle, Birmingham B47ET, UK

<sup>e</sup> Dipartimento di Chimica "Ugo Schiff" and CSGI, Università degli Studi di Firenze, Via della Lastruccia 3, 50019 Sesto Fiorentino, Italy

## ARTICLE INFO

### Keywords:

Plasmonics  
Fibre optics  
Nanostructures  
Bisphenol A  
Aptamers  
Biosensors

## ABSTRACT

We present a plasmonic biosensor capable of detecting the presence of bisphenol A in ultra-low concentrations, yielding a wavelength shift of  $0.15 \pm 0.01$  nm in response to a solution of 1 fM concentration with limit of detection of  $330 \pm 70$  aM. The biosensing device consists of an array of gold nano-antennae with a total length of 2.3 cm that generate coupled localised surface plasmons (cLSPs) and is covalently modified with an aptamer specific for bisphenol A recognition. The array of nano-antennae is fabricated on a lapped section of standard telecommunication optical fibre, allowing for potential multiplexing and its use in remote sensing applications. These results have been achieved without the use of enhancement techniques and therefore the approach allows the direct detection of bisphenol A, a low molecular weight (228 Da) target usually detectable only by indirect detection strategies. Its detection at such levels is a significant step forward in measuring small molecules at ultra-low concentrations. Furthermore, this new sensing platform paves the way for the development of portable systems for in-situ agricultural measurements capable of retrieving data on a substance of very high concern at ultra-low concentrations.

## 1. Introduction

Over the last couple of decades there has been a growing concern about the increasing concentration of various endocrine disruptive compounds (EDCs) within the environment. These compounds have been identified as “substances of very high concern” by various governing bodies across the globe, such as the European Chemicals Agency (ECHA) (Ash and Ash, 1995). EDCs can potentially affect both human health and wildlife, altering early development and impairing adult life functioning in individuals, as well as whole populations and local communities. Bisphenol A (BPA) is an EDC included in the group of xeno-estrogens, which is used in the fabrication of epoxy coatings and polycarbonate. Endocrine disruption by BPA happens when the molecule binds estrogen receptors, which has been shown to produce reproductive abnormalities in wildlife (Segner et al., 2003). Furthermore, BPA may induce a decrease of sperm quality in humans (Toppari et al., 1996; Vandenberg et al., 2007). A particularly alarming feature of BPA is that even at very low concentrations, this compound has shown the

potential to produce adverse effects such as reproductive disorders, chronic diseases, and various types of cancer in in-vitro animal models (Oppeneer and Robien, 2015; Huo et al., 2015). As a consequence, both Canada and China banned the use of BPA in baby bottles in 2010 and 2011 respectively. There is growing concern regarding the build-up of EDCs in the environment especially in regard to agricultural areas, which can act as a gateway for EDCs to enter the food chain. BPA has become a widespread contaminant, and is present in wastewater (Furhacker, 2000), river water, and sediments (Boltz et al., 2001; Fromme et al., 2002), ranging from  $\mu$ M concentrations in raw sewage or wastewater effluents (Heemken et al., 2001) and reducing to nM concentrations in river water and sediments (Fromme et al., 2002). Furthermore, there are some results that suggest that BPA may also mimic the action of thyroid hormone (Watabe et al., 2004).

The potential deleterious effects of EDCs provide governments and health regulators with much cause for concern, due to the fact that these substances are commonly used in the production of a variety of plastics, such as, polyvinyl chloride (PVC) (Ash and Ash, 1995), widely

\* Corresponding author.

E-mail addresses: [t.d.p.allsop@aston.ac.uk](mailto:t.d.p.allsop@aston.ac.uk), [tomallsop@io.cfm.csic.es](mailto:tomallsop@io.cfm.csic.es) (T.D.P. Allsop), [wangc15@aston.ac.uk](mailto:wangc15@aston.ac.uk) (C. Wang).

<https://doi.org/10.1016/j.bios.2019.02.043>

Received 6 November 2018; Received in revised form 10 February 2019; Accepted 15 February 2019

Available online 22 February 2019

0956-5663/ © 2019 The Authors. Published by Elsevier B.V. This is an open access article under the CC BY-NC-ND license (<http://creativecommons.org/licenses/by-nc-nd/4.0/>).

present both in industry and private households. Some of these materials are used in containers that store or carry both food and water.

Although there are a variety of methods used to detect BPA, most are cumbersome and laboratory-based, in addition to being time-consuming as well as expensive (Moriyama et al., 2002). Among the most common methods to determine the presence and concentration of BPA in environmental samples are the use of high-pressure liquid chromatography (HPLC) (Vandenberg et al., 2007), liquid chromatography (Oppeneer and Robien, 2015), and gas chromatography (Huo et al., 2015) coupled with mass spectrometry. These techniques are typically slow in turnaround, and cannot be taken to the field, so they cannot perform on-site measurements. Furthermore, they are complex, requiring highly skilled operators.

The static nature of current detection techniques and their requirement for skilled input underlines the urgent need for an as-of-yet unavailable portable, easy to operate, cost-effective and robust sensing scheme capable of detecting ultra-low concentrations of BPA in the agricultural and food industry. Therefore, recent research has focused on finding a more portable technique (Ragavan et al., 2013; Mei et al., 2013). Due to the interest in producing a portable sensing scheme while keeping high analytical performances, biosensors, including surface plasmon resonance (SPR), are researched as a possible solution working in conjunction with selective recognition receptors. Among currently used receptors, the synthetic ones display the ideal features for miniaturized and portable biosensors, especially aptamers, peptides, and molecularly imprinted polymers.

In this paper, the authors present results of the development of an affinity-based optical aptasensor based upon a nanostructured antenna arrayed to create a plasmonic sensing platform on optical fibres. Using a simple interrogation scheme, this sensing platform was able to detect the small molecule bisphenol A at a concentration of 1 fM yielding a wavelength shift  $0.15 \pm 0.01$  nm, suggesting a limit of detection (LOD) of  $330 \pm 70$  aM solution in standard solutions. This represents a significant decrease in the LOD with respect to other reported immunosensors, by several orders of magnitude, representing a significant step forward in the detection of small molecules at ultra-low concentrations. Furthermore, this sensing platform has the potential to be made portable and simple to operate, thus offering the opportunity to make a portable system for in-situ agricultural measurements, to amass data on a substance of very high concern at ultra-low concentrations.

## 2. Experimental

### 2.1. Materials and methods

The bare optical fibre, that were side-polished, were purchased from **Phoenix Photonics Ltd**, Birchington, Kent, UK, and was specified as type SMF28. The side polishing produces a flat D-shaped fibre with the flat of the D shaped fibre is 3  $\mu$ m with the cladding/core interface.

The multi-layered coatings were deposited using a Nordico 6 in. RF/DC 3 target excitation machine, (Nordiko Technical Services Limited, Havant, Hampshire, UK). The Sputtering targets were supplied by Goodfellow Cambridge Ltd, The specification of the sputtering targets was: Au, High Purity: 99.999%, Ge Purity: 99.999%, SiO<sub>2</sub> Purity: 99.995%.

The UV processing is performed using an optomechanical apparatus used for the fabrication of conventional phase mask Fibre Bragg gratings. The UV light source is an Argon ion laser producing irradiance at 244 nm, the laser used 0.5 W INNOVA Sabre FReD with beam waist of 0.65 m, **Coherent Inc**, Santa Clara, CA, USA. The phase masks have a period of 1.018  $\mu$ m and were manufactured by **QPS Photonics Inc**, Quebec, Canada, and the motorised mechanical supplied by **Aerotech Inc**, Pittsburgh, PA, USA.

All chemicals used in the assessment of the performance of the biosensor to detect and its chemical selectivity were supplied by **Sigma-Aldrich/Merck KGaA**, Darmstadt, Germany specifically Bisphenol A,

Purity:  $\geq 99\%$ , Bisphenol B Purity: analytical standard, the various concentration were produce using the logarithmic dilution method. **Aston University** produced TRIS buffer solution, tris(hydroxymethyl) aminomethane (HOCH<sub>2</sub>)<sub>3</sub>CNH<sub>2</sub> along with the 4 M solution of NaCl

The refractive index spectral sensitivities were estimated by submerging the biosensors into standardised solution ranging from n<sub>D</sub> 1.300–1.395, Adjustment  $\pm 0.0002$  supplied by **Cargille-Sacher Laboratories Inc**, Cedar Grove, NJ, USA Refractive Index Matching Liquids, series AAA: Range n<sub>D</sub> 1.300–1.395,...

### 2.2. Fabrication of LSPs sensors

A series of four sensors were fabricated in four stages and after each stage the sensors were calibrated for refractive index and polarisation spectral sensitivity. Stage one of fabrication was the lapping of SMF 28 standard telecoms optical fibres to produce a D-shaped cladding optical fibre where the flat surface of the D cladding is 3  $\mu$ m from the core/cladding interface (purchased from Phoenix Photonics Ltd). In the second stage of fabrication, the layer-to-layer deposition of germanium (36 nm), silicon dioxide (24 nm) and gold (22 nm) onto the flat of the D-shaped cladding was accomplished. The thicknesses have been chosen to maximise the coupling of surface plasmons in the 1200–1600 nm region of the spectrum, as justified elsewhere (Allsop et al., 2009). The thin films were deposited using an RF sputtering machine (Nordico 6 in. RF/DC 3 target excitation machine, Nordiko 6, Nordiko Technical Services Limited, Havant, Hampshire, UK). The third stage of the fabrication procedure was the creation of the low dimensional nanostructured coating by spatially aligning the flat of the D-shaped fibres, so they were then exposed to various intensities of an UV beam at 244 nm (Argon ion laser, INNOVA Sabre Coherent inc.). The opto-mechanical arrangement of the apparatus is the same for the UV inscription of optical fibre gratings (Bennion et al., 1996). The UV beam was focused along the line of travel of the air-bearing stage (using a plano-convex lens focal length of 80 mm), then passed through a phase mask (period of 1.018  $\mu$ m). The beam was then focused in two axes parallel and perpendicular to line of travel of the air-bearing stage (using two plano-convex lens both having focal lengths of 80 mm).

### 2.3. Modification with aptamer and bisphenol A measurements

The LSP sensors were covalently modified with a DNA aptamer selected for the capturing of PBA in solution, and available from literature (Jo et al., 2011). The immobilisation was carried out by dipping the fibres singularly in an aqueous solution of 1 M KH<sub>2</sub>PO<sub>4</sub> pH = 3.5 containing the aptamer (1  $\mu$ M) for 16 h. In these conditions, the 5' thiol moiety of the aptamer is covalently bound to the gold surface in an irreversible manner. After incubation, the aptamer solution was removed and replaced with a 1 mM ethanol solution of 6-mercaptohexanol to passivate the gold surface not covered by the aptamer. Finally, the sensors were washed and stocked in 1 M KH<sub>2</sub>PO<sub>4</sub> pH = 3.5 as a maintaining solution. The tubes were sealed and stored at 4 °C until use.

Since the 90's, aptamers have emerged in literature as possible alternative to antibodies in biosensing. At present, their selection, characterisation, and binding mechanisms are well-established aspects widely reported in literature. The aptamer selected for biosensing experiments in this article has been selected from the literature (Jo et al., 2011) where authors deeply characterised the kinetic parameters.

### 2.4. Optical set up

The experimental apparatus for the characterisation of the sensors is shown in Fig. 1a. The refractive index characterisation is done by immersing the sensors into certified refractive index liquids (Cargille-Sacher Laboratories Inc.) that have a quoted accuracy of  $\pm 0.0002$  situated on an aluminium plate in a V-groove, the plate being machined flat to minimise bending of the fibre. The plate was placed on an optical

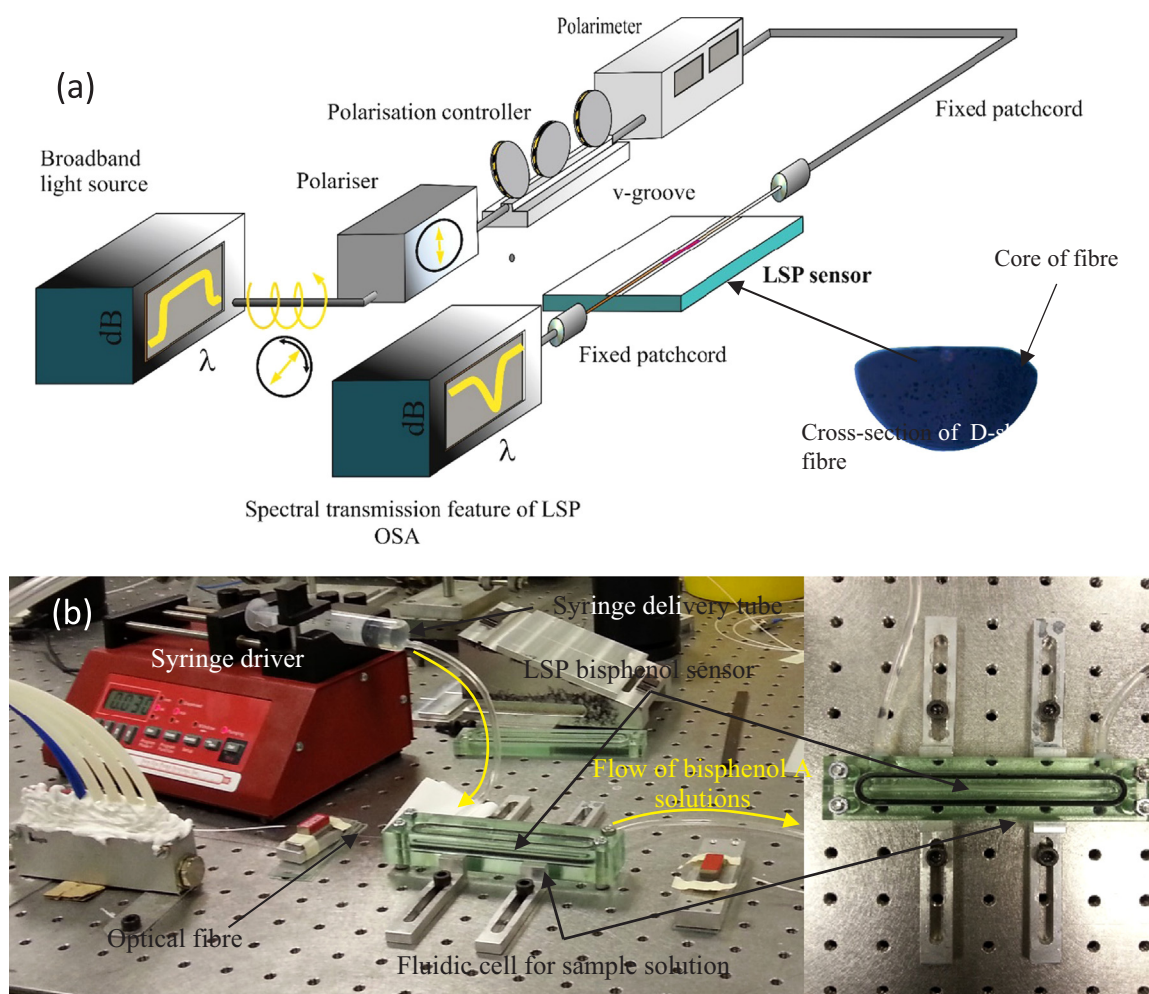


**Fig. 1.** (a) The characterisation apparatus for the LSP sensors. (b) Image of the handling and solution sample delivery system.

table, which acted as a heat sink to help maintain a constant temperature throughout the experiments. Furthermore, the sensor is illuminated with polarised light, such that the polarisation state of the light yields a maximum optical strength transmission resonance. This is achieved by a broadband light source in conjunction with a broadband linear polariser and a polarisation controller. The apparatus used for measurements of bisphenol A is based on that shown in Fig. 1a, with the inclusion of a programmable syringe driver (NE1002X -microfluidic syringe pump, Scientific Instrument Service Inc.), equipped with two isolation valves on the delivery tube to the import port and on the exit port of the fluidic cell to hold and immerse the sensor. The maximum volume of solution contained in the cell is 1.9 ml, see Fig. 1b.

There was a particular protocol used with the fluidic cell and syringe driver: the initial wash is with TRIS buffer solution, then a distilled water wash, followed by the bisphenol A solution at a rate of 0.5  $\mu\text{l}/\text{min}$  and then a further two wash cycles, first with distilled water followed with a TRIS buffer solution and then using a 4 M solution of NaCl for regeneration. The syringes used in the experiments are used only once to ensure there is no cross-contamination between the liquids. During a single experiment the sensor is always immersed in a liquid; during the changing of syringes both isolation valves on the import and exhaust are closed to ensure the sensor remains immersed.

## 2.5. Measurements of bisphenol A samples

To assess the sensitivity of the sensors a series of BPA solutions in water ranging from 10 nM to 1 fM were tested in triplicates. The

protocol used for the series experiments involving the bisphenol solutions is as follows: an initial wash with TRIS buffer solution (50 mM Tris, 140 mM NaCl, 1 mM  $\text{MgCl}_2$ , pH 7.4,) was performed, followed by a distilled water wash; then the bisphenol A solution was delivered at a rate of 0.5  $\mu\text{l}/\text{min}$  and then a further two wash cycles, firstly with distilled water followed by TRIS buffer solution. Finally, a 4 M solution of NaCl was injected for regeneration. The syringes used in the experiments are used only once to ensure there is no cross-contamination between the liquids. During a single experiment the sensor is always immersed in a liquid; during the changing of syringes both isolation valves on the import and exhaust are closed to ensure the sensor remains immersed. Negative control measurements were carried out with bisphenol B under the same binding conditions.

Typical experimental results of the lapped fibres for index and polarisation spectral sensitivity are reported in Fig. 2a to d which show that light is being out coupled at high refractive indices with a maximum DC out-coupling of  $-4.7$  dB over the wavelength range when being immersed into a solution with an index of 1.38 and above, and that there is variation in out-coupling occurring with the polarisation of the illuminating light, with a maximum of  $-6.2$  dB occurring with polarisation perpendicular to the flat of the D shaped cladding. The last result, the transmission features, are attributable to the asymmetry of the fibre due to the lapping, see Fig. 2c and d.

The gold is chosen for the metal overlay coating for three reasons. Firstly, it is a metal and will support surface plasmons. Secondly, the gold will yield a surface plasmon with maximum spectral sensitivity in the aqueous index regime. Thirdly, gold-thiol chemistry is used for the



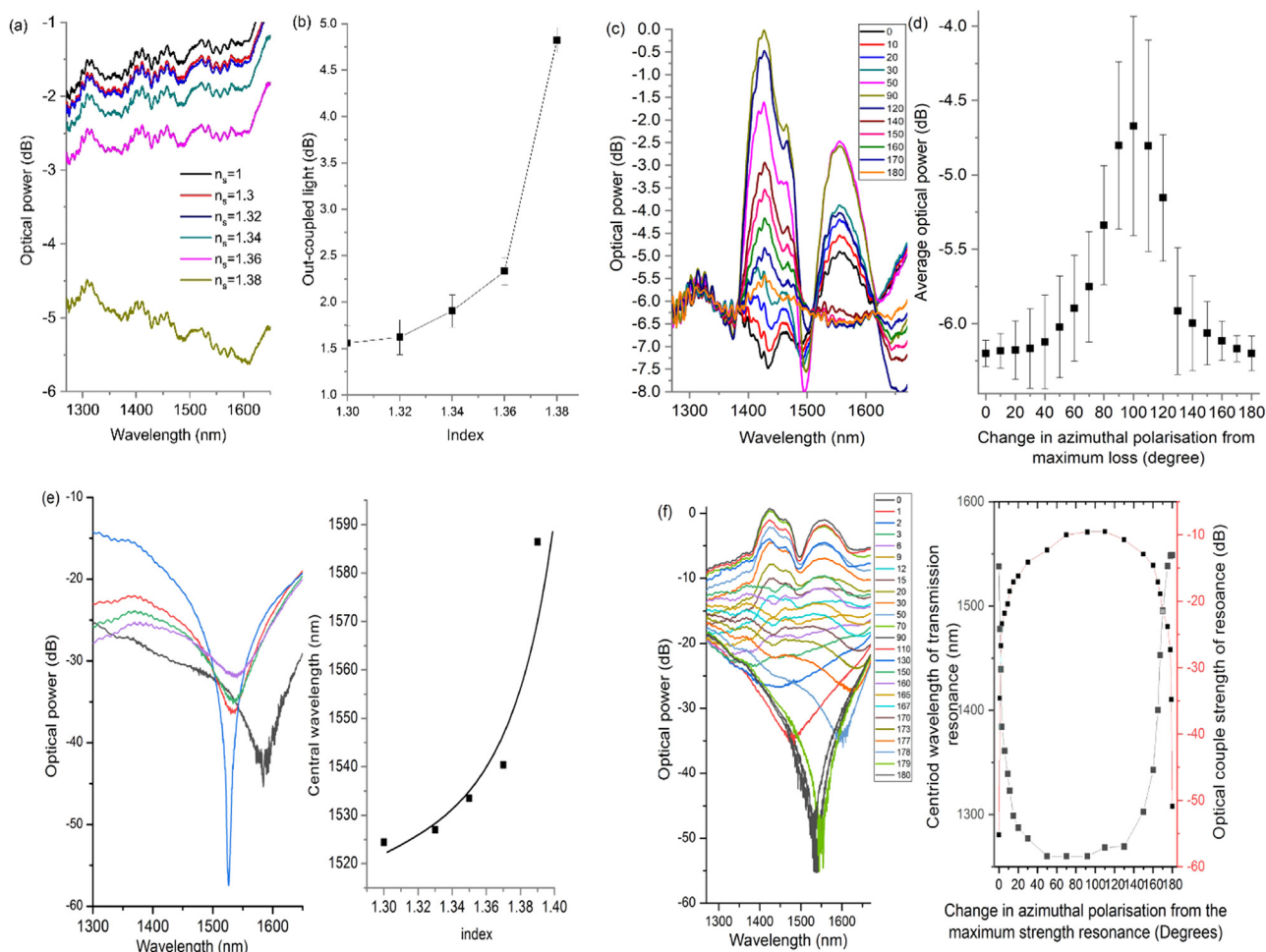


**Fig. 2.** Typical refractive index (a,b) and polarisation (c, d) spectral properties of the D-shaped fibre used to fabricate the LSP sensors. (a) transmission spectrum and (b) spectral sensitivity with respect to refractive index of the surrounding medium (c) transmission spectrum and (d) spectral sensitivity with respect to the change in azimuthal polarisation of the illuminating light with maximum of coupling at 0 degree of the azimuthal polarisation. (e) typical refractive index and polarisation spectral properties of the D-shaped fibre with a multi-layered coating consisting of germanium, silicon dioxide and gold with thicknesses of 36 nm, 24 nm and 22 nm respectively, used to fabricate the LSP sensors transmission spectrum and spectral sensitivity with respect to refractive index of the surrounding medium with a maxima of coupling strength in air. (f) LSP transmission spectrum and spectral sensitivity with respect to the change in azimuthal polarisation of the illuminating light with maximum of coupling at 0 degree of the azimuthal polarisation.

immobilisation of the aptamer on the surface of the fibre. The other materials are used to create the nano-antennae array using the 244 nm UV irradiance.

Typical experimental results for refractive index and polarisation sensitivity for this combination of fibre and multi-layered coating are shown in Fig. 2e and f. The recorded samples shown index sensitivities of  $\sim 10^3$  nm/RIU. In Fig. 2e this value is approximately  $\sim 1200$  nm/RIU, with a maximum polarisation sensitivity of 2 nm/degree

The coupled LSP optical fibre sensing platform is created by illuminating the multi-layered optical fibre with UV (244 nm) irradiance. This creates an array of nano-antennas, see Fig. 3a–d, which have been studied and reported elsewhere (Allsop et al., 2012). The surfaces were investigated with atomic force microscopy (AFM), X-ray photoelectron spectroscopy (XPS) and using a spectroscopic ellipsometer (SE) (Allsop et al., 2012). In summary, AFM revealed a corrugated surface in which the apex of each corrugation was made of gold and surrounded by dielectric materials with a repeatable structure over centimetres. Typically, the radius of the gold stripes/antennae was 80 nm with a length of 20  $\mu$ m and a period of 530 nm.

As in each previous step, the obtained devices were characterised with respect to index and polarisation, see Fig. 4a and b. Furthermore, the UV processing has increased significantly the refractive index spectral sensitivity from the  $\sim 10^3$  nm/RIU to  $\sim 7 \times 10^3$  nm/RIU. An

increase in polarisation dependence with a maximum polarisation sensitivity of 15 nm/degree is also obtained, as expected. In fact, the physical mechanism for the dramatic increase in spectral sensitivity is caused by the significant increase in the interaction length of the infrared surface plasmons caused by the strong coupling between adjacent localised surface plasmons supported on an array of nanoscale antenna-like structures.

### 3. Results and discussion

To assess the sensitivity of the sensor a series of BPA solutions in water ranging from 10 nM to 1 fM were tested. Below are representative spectral responses of the response of these sensors to various concentrations of bisphenol A solutions, 1 fM, 100 fM, 100 pM and 1  $\mu$ M, see Fig. 5. The results for individual sensor trials are shown in Fig. 6.

To assess the chemical functionality with regards to the chemical selectivity of the aptasensors to bind to bisphenol A ( $C_{15}H_{16}O_2$ ), series of tests were performed with various concentrations of bisphenol B ( $C_{16}H_{18}O_2$ ) solutions. This particular compound was chosen because of its similar size; bisphenol B is, 242 Da to 228 Da, although of course the chemical functionality is different due to the different chemical structure and shape. The various concentrations of solutions of bisphenol B were produced by the logarithmic dilution technique, starting with a

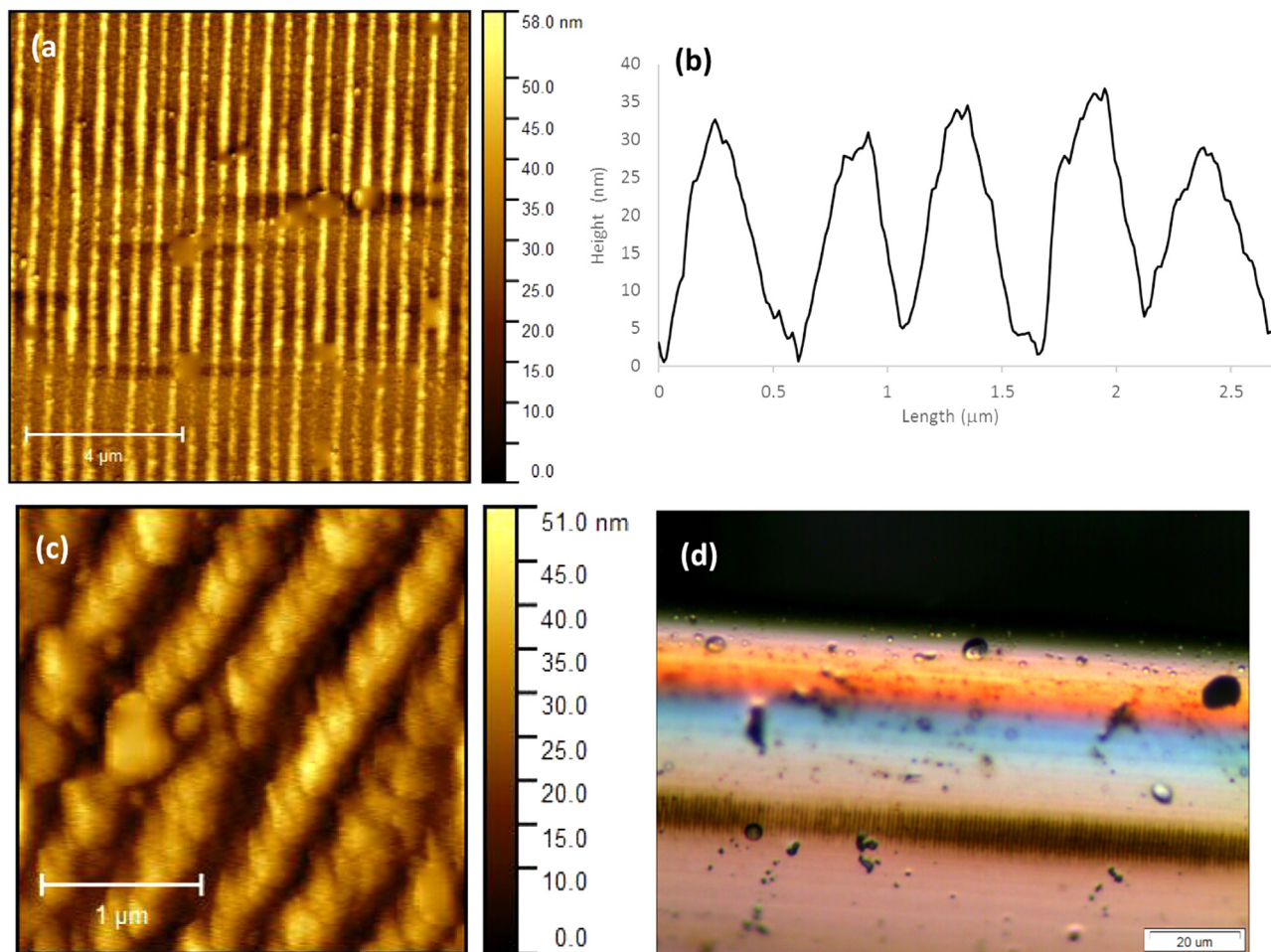


**Fig. 3.** Typical surface profiles and images of the LSP sensor, (a) AFM image of the flat of the D-shaped UV processed coated fibre and the repeatable fabricated structure. (b) Line profile of an AFM image showing the cross-sectional view of the corrugation created on the surface. (c) High resolution AFM image of the UV processed surface. (d) optical microscope image of the flat of the D-shaped fibre showing the surface corrugation.

solution concentration of 1  $\mu\text{M}$  and down to 1 fM. The same test procedure was adopted for all the bisphenol B solutions as for the bisphenol A. The aptasensors produced no negligible results for both changes in optical strength or wavelength shift for all the

concentrations used for bisphenol B solutions. The highest concentration for bisphenol B is shown in Fig. 5a and b.,

A summary of the results is displayed in Fig. 6(a) to (c), showing that the wavelength interrogation scheme with 1 fM solution of

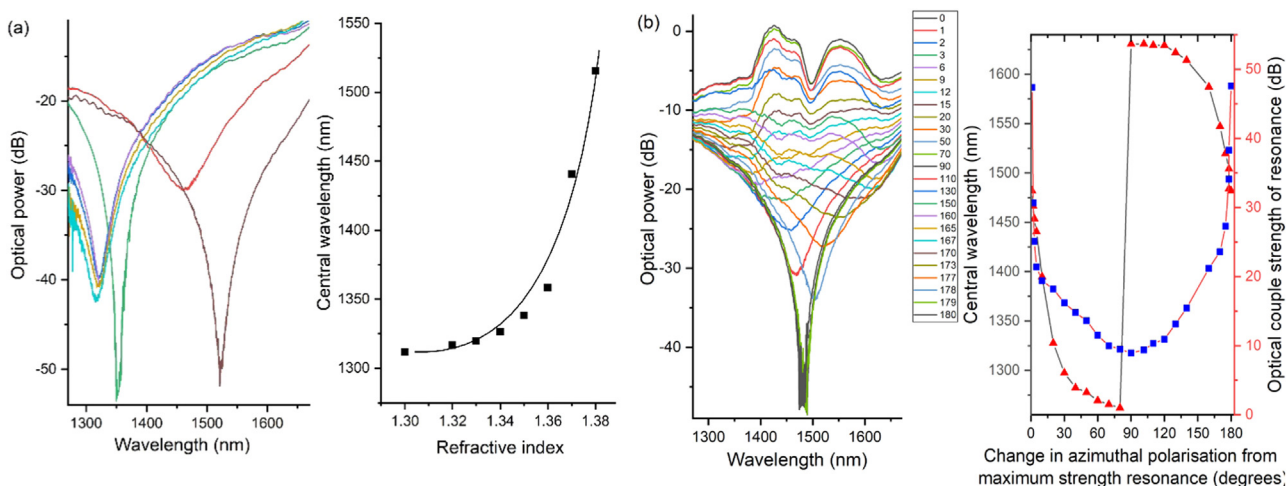


**Fig. 4.** Typical refractive index and polarisation spectral properties of the D-shaped fibre after multi-layered coating and UV processing to produce the LSP sensing platform. (a) Transmission spectrum and spectral sensitivity with respect to refractive index of the surrounding medium with a maximum of coupling strength in air (b) Transmission spectrum and spectral sensitivity with respect to the change in azimuthal polarisation of the illuminating light with maximum of coupling at 0 degree of the azimuthal polarisation.

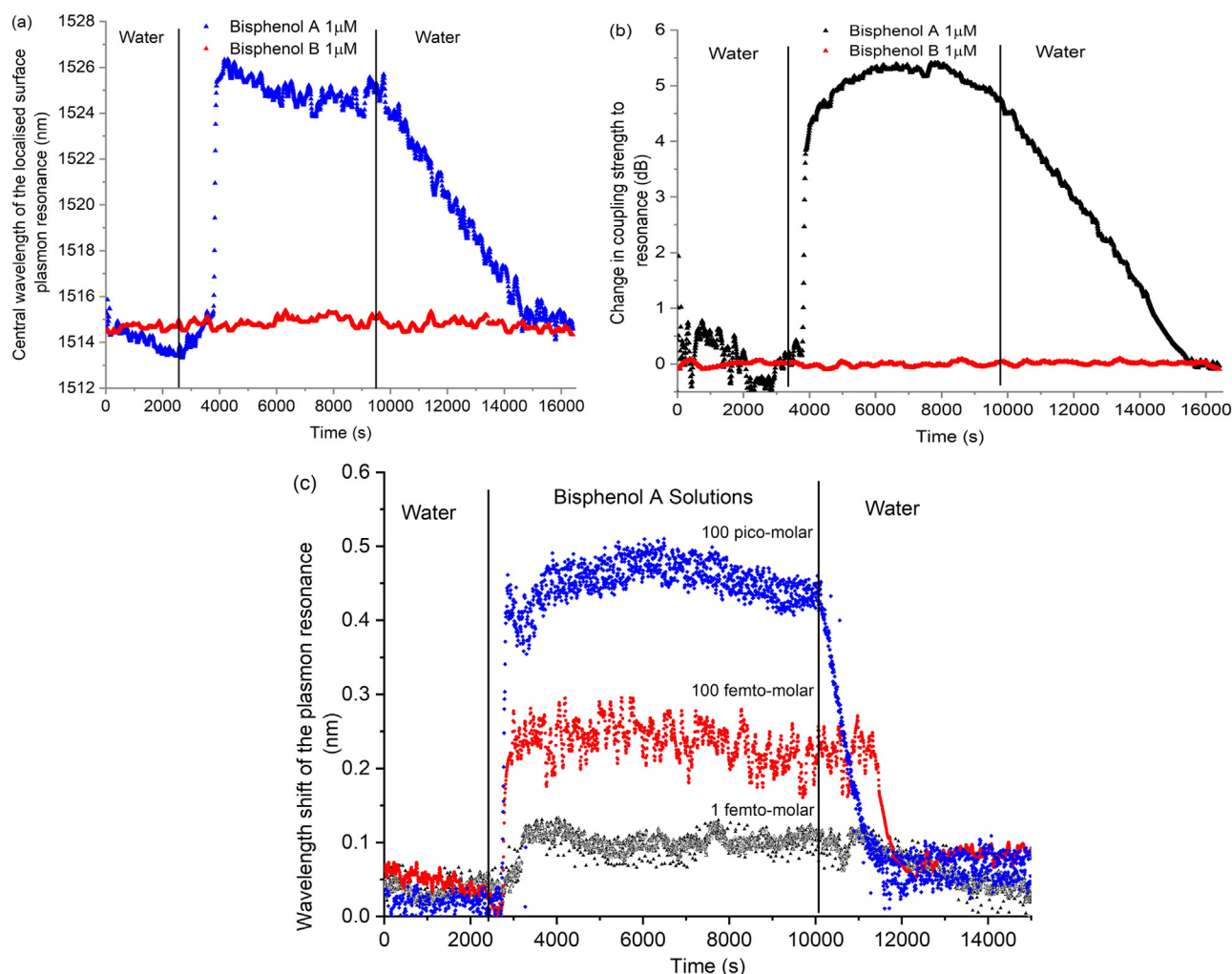


**Fig. 5.** Typical examples of the wavelength shift response of the plasmonic sensors using the flow cell, showing association and dissociation of the bisphenol A with the aptamer, the biosensor results for both wavelength shift (a) and the change in optical strength (b) with a 1  $\mu\text{M}$  solution along with the results obtained with a 1  $\mu\text{M}$  solution of bisphenol B. (c) Typical results with various bisphenol A solutions with differing concentrations: 1 fM ( $\blacktriangle$ ), 100 fM ( $\bullet$ ) and 100 pM ( $\blacklozenge$ ).

bisphenol produces a wavelength shift of  $0.15 \text{ nm} \pm 0.01 \text{ nm}$ . Using a linear regression yields a limit of detection of a solution concentration of 330 aM, but inspecting Fig. 6, the intrinsic wavelength error within the signal is  $\pm 0.01 \text{ nm}$  which leads to an error estimate in concentration of  $\pm 70 \text{ aM}$ , thus leading to an LOD of  $330 \pm 70 \text{ aM}$  solution. These data are inferred from independent measurements on four devices and over a series of 12 different experiments over the range of concentrations. From these experiments the estimated pooled repeatability standard deviation is  $\pm 80 \text{ aM}$  between sensors and the intra-reproducibility within all the experiments for a sensor yielded a variance of  $\pm 44 \text{ aM}$  between the estimated LODs. This limit of detection is complicated to estimate due to the increasingly stochastic nature of the response of the system at these ultra-low concentrations and thus a conventional limit of detection may be misleading. The optical strength yields a detection limit at least one order magnitude higher in concentration, see Fig. 6a and b. This would be expected due to the fact that the phase-matching condition is more sensitive to medium changes than the coupling efficiency of the localised surface plasmons as they are governed by different mechanisms (Brockman et al., 2000; Patskovsky et al., 2003; Spoto and Minunni, 2012).

Furthermore, looking at the incubation times, as shown in Fig. 6c, there appears to be a similar behaviour observed when this sensing approach is used for another target molecule, thrombin (Allsop et al., 2017). In particular, the major difference is the “up-turn” in the incubation that occurs at molar concentrations of  $10^{-14}$  for the bisphenol

A, compared to  $10^{-16}$  for thrombin which is an approximately two orders larger in size to bisphenol A, i.e. 228 Da (size  $\sim 0.1 \text{ nm}$ ) to 37 kDa (size  $\sim 5 \text{ nm}$ ), respectively. This is suggesting that the kinetics of ultra-low concentrations of molecules are having some common physical manifestation that is being governed by stochastic binding events; the behaviour is being investigated by the authors. There are many approaches to estimate the performance and to assist in the understanding of the sensing platform; one such procedure is the concentration-response curves shown in Fig. 6d and e for both change in wavelength and optical strength of the LSP resonance in the transmission spectra.

Inspecting Fig. 6d and e, an estimate of the half maximal effective concentration,  $\text{EC}_{50}$ , (Alexander et al., 1999) can be made leading to  $1.8 \pm 0.3 \text{ nM}$  and  $72.5 \text{ nM}$  for wavelength and optical strength, respectively. Considering the wavelength shift, this also is defined at the equilibrium dissociation constant;  $K_D$  and its reciprocal value being the equilibrium association constant  $K_a = 5.6 \times 10^8 \text{ M}^{-1}$ . Furthermore, Using the combined experimental data and the pseudo first-order kinetics approximation for the reaction, the association and dissociation rate constant were determined graphically, yielding an association rate constant of  $4.151 \times 10^8 \text{ M}^{-1} \text{ s}^{-1}$ , which leads to a dissociation rate constant of  $7.472 \times 10^{-3} \text{ s}^{-1}$ . Comparing these determined kinetic constants to those in the literature, (Marks et al., 2014), firstly it was noted that the dissociation constant in the literature ranged from  $\sim 54\text{--}0.7 \text{ nM}$ . The higher value of dissociation constant was obtained with a method that had a relatively high limit of detection, a value of



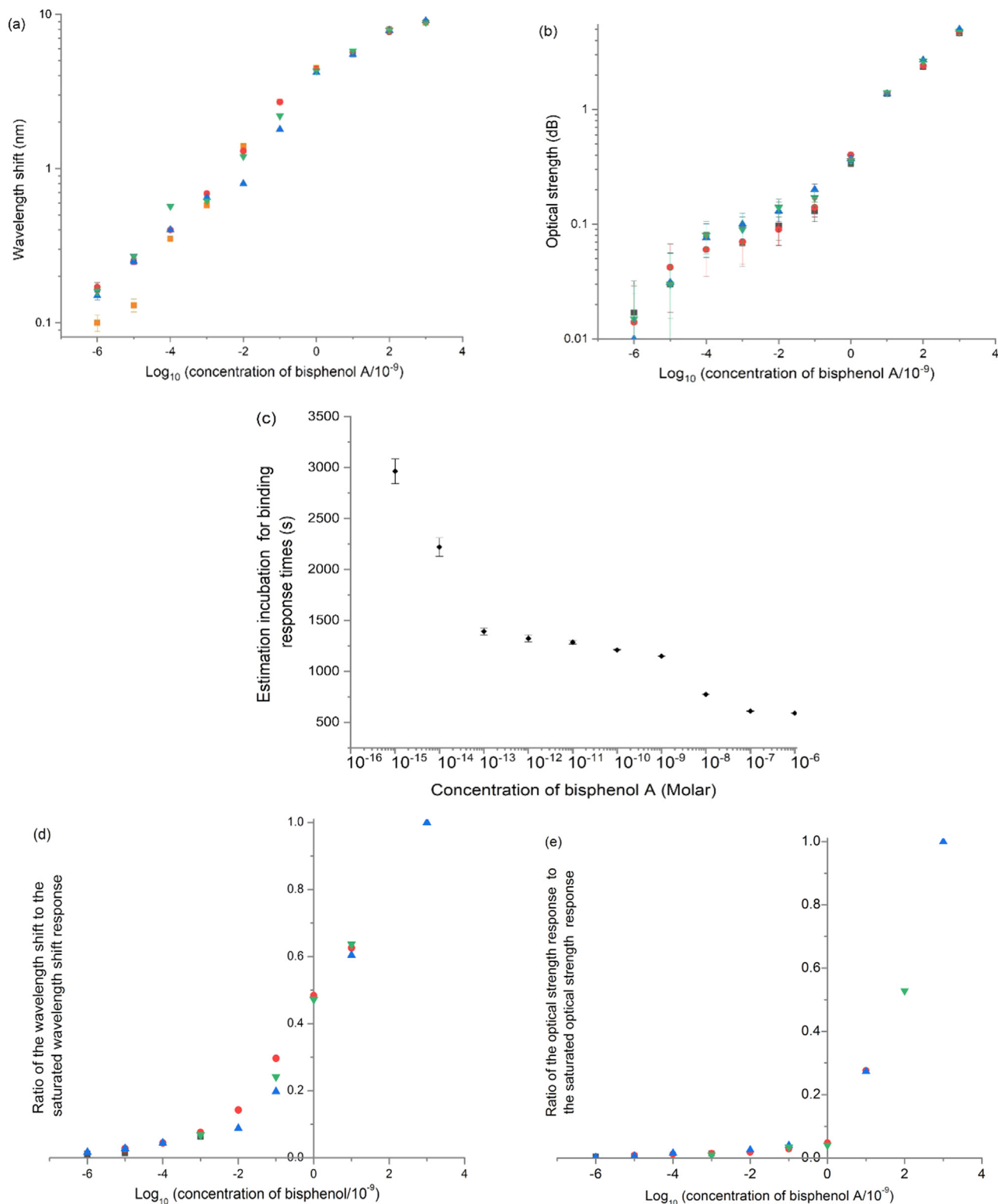


**Fig. 6.** Spectral sensitivity of aptamer-coated, multilayered LSP fibre devices. (a) wavelength shifts as a function of bisphenol A concentration. (b) Change in optical coupling strength as a function of bisphenol A concentration. In figures (a) & (b), ●, ▲, ▼ and ■ represent measurements made with four different devices. (c) Estimation of incubation times of the binding reaction as a function of bisphenol A concentration obtained from four different devices over 12 experimental trials, the associated errors are the standard deviations calculated for each experiment at each concentration. (d) Concentration-response curves based upon wavelength shifts changes for bisphenol A concentrations. (e) Concentration-response curves based upon optical strength changes for bisphenol A concentrations.

3 nM. We had obtained similar results to other researchers (Hayat and Marty, 2014; Xiao et al., 2008), quoting a dissociation constant of 0.7 nM and 0.8 nM respectively. Furthermore, a similar high equilibrium association constant to other researchers,  $2.1 \times 10^7 \text{ M}^{-1}$  (Ma

et al., 2017).

We found that the devices had a saturation concentration of  $1 \mu\text{M}$  and produced a maximum wavelength shift of  $9.630 \pm 0.008 \text{ nm}$  and  $5.027 \pm 0.015 \text{ dB}$  change in optical strength. Using the data collected

and the stated maximum responses, it was determined that this mechanism is a negatively cooperative binding; once the target molecule is attached to the receptor, the affinity for other target molecules decreases. This was deduced from the Hill coefficient for the equilibrium yielding  $n_{H\text{intensity}} = 0.273$  and  $n_{H\text{wavelength}} = 0.318$ , respectively, which was estimated using the standard graphical approach (Attie and Raines, 1995). Whilst the above  $EC_{50}$  values and the aforementioned detection limit is debatable as a performance estimate of a detection scheme, another approach is to use the  $EC_{10}$  value to yield an estimate of detection using  $EC_A = (A/(100 - A))^{1/n_H} EC_{50}$  where  $A$  is the desired effective concentration and  $n_H$  is the Hill coefficient (determined experimentally). Thus the  $EC_{10}$  point is  $1.845 \pm 0.006$  pM and  $25.03 \pm 0.01$  pM for wavelength and optical strength, respectively, which is comparable to optical immunosensors, which provide lower limits of  $\sim 0.2$  pM (Mei et al., 2013). The authors would like to state that  $EC_{10}$  is commonly used as a measure of a drug's potency and not the general used by experts in photonics. Along with these already mentioned attributes, there is another of particular interest called surface coverage resolution (Homola, 2008), i.e. the minimum identifiable valid change of molecular mass captured by the recognition molecule. The coverage can be defined as  $\sigma_T = \sigma_N h / \left( \frac{\Delta\lambda}{\Delta n} \right) \cdot \left( \frac{\Delta n}{\Delta c} \right)$  where  $\sigma_N$  is the associated noise within the result (0.02 nm),  $h$  is the thickness of the layer that has the refractive index change associated with the aptamer molecule (assumed here to be of the order of the size of the bisphenol A molecule, 0.1 nm), and  $\Delta n/\Delta c$  is the volume refractive index increment of the molecular concentration that has typical values ranging from 0.1 to  $0.3 \text{ cm}^3/\text{g}$  (Homola, 2008), taking the mid-point leads to  $0.043 \text{ pg}/\text{mm}^2$ . This result is the highest from an optical sensing platform reported in the literature by an order of magnitude (Aghamiri et al., 2018; Ermini et al., 2013; Lee et al., 2009; Santos et al., 2018).

There are several aspects of this biosensor that need to be discussed and compared to the present state of the art on bisphenol A detection in general and with optical/photonic techniques. Firstly, the conventional methods to determine the presence bisphenol A, HPLC and liquid/gas chromatography, can detect the bisphenol A at ultralow concentrations but they are more difficult to implement for in-situ environmental measurements at present. In recent years, immunochemical methods have been used with limit of detection down to 200 pM concentrations (Furhacker et al., 2000), again these methods are laboratory based and time consuming. Typically, electrochemical immunosensors for the detection of bisphenol A yield limits of detection ranging from 4 nM to 10 fM, and optical immunosensors of  $\sim 60$  nM (Rodriguez-Mozaz et al., 2005). Comparing the results obtained in this work; a limit of detection of  $330 \pm 70$  aM, to the quoted limits of detection in the literature, there is an order magnitude increase in limit of detection, with a Figure-of-Merit (Allsop et al., 2009) (FOM) of 88. The  $FOM = (\Delta\lambda/\Delta n)/\Delta\lambda_{FWHM}$ , where  $\Delta\lambda_{FWHM}$  is the full width at half maximum of the spectral feature. The index resolution is determined in part by the utilized interrogation scheme, which in this case is an optical spectrum analyser (OSA) that has 1000 measurable points over the FWHM of the resonance (80 nm), leading to a measurement resolution of  $\sim 0.1$  nm (which is the resolution of the OSA). The FOM value for this sensing platform is reasonably good and has a typical mid-range value compared to other sensing systems (Allsop et al., 2009; Allsop et al., 2017; Attie et al., 1995; Yesilkoy et al., 2018). A broader comparison against other techniques, such as impedimetric/electrically based sensing schemes, shows this plasmonic scheme presented in this work has the lowest measured limit of detection, typically the electrically based systems yield fM to few nM, (Mirzajani et al., 2017) plus references therein and (Zheng et al., 2018). Furthermore, the surface coverage resolution of  $0.043 \text{ pg}/\text{mm}^2$  for bisphenol A for this sensing platform for a molecule size of 230 Da is being compared where the majority of previous reported work are detecting molecules of sizes from 6 kDa to 200 kDa with coverages ranging a few to approximately one  $\text{pg}/\text{mm}^2$  for large molecules (tens kDa) (Liu et al., 2018) and for a smaller

molecule  $0.96 \text{ pg}/\text{mm}^2$  has been reported (Aghamiri et al., 2018) which as a lower resolution by over a factor of 20. This sensor is regenerated using a very simple wash and has the potential to be made small and portable.

#### 4. Conclusions

In conclusion, this is the first small molecule plasmonic biosensor to achieve a measured LOD in the attomolar concentration range. It does so with molecule sizes smaller by approximately two orders of magnitude with respect to other low-concentration sensors. Specifically, it provides the highest measured resolution ever obtained for bisphenol A and it offers the additional advantage of having a very simple operating procedure. Along with having the best the surface coverage resolution performance reported in the literature. The results presented here demonstrate that this novel localised surface plasmon sensing platform, when combined with the recognition aptamer molecule, can offer a new detection paradigm for small molecules, paving the way to portable on-site tests with performances that can easily match those currently only achievable in the laboratory.

#### Author statement

Each of the authors contributed as following: Thomas D. P. Allsop developed the original plasmonic concept. Thomas D. P. Allsop modelled, designed and performed experiments, analysed the data for the plasmonic devices. Thomas D. P. Allsop, Changle Wang, Ronald Neal fabricated the plasmonic devices. Simona Scarano and Maria Minunni developed mobilisation procedure of the aptamer and adhered the aptamers to the plasmonic devices. David A. Nagel and Anna V Hine prepared solutions for experiments. Thomas D. P. Allsop developed the explanation for sensor behaviour and performed experiments. The manuscript was written by Thomas D. P. Allsop, Anna V Hine, David A. Nagel, David J. Webb, Ronald Neal, Philip Culverhouse, Simona Scarano, Maria Minunni, Juan D. Ania Castañón. All authors discussed the results and commented on the manuscript.

#### Acknowledgments

Each of the authors contributed as following: T. A. developed the original plasmonic concept. T.A. modelled, designed and performed experiments, analysed the data for the plasmonic devices. T.A., C.W., R.N. fabricated the plasmonic devices. M. M. and S.S. developed mobilisation procedure of the aptamer and adhered the aptamers to the plasmonic devices. D. N. and A. V. H. prepared solutions for experiments. T. A. developed the explanation for sensor behaviour and performed experiments. The manuscript was written by T.A., A.V. H., D. N., D.J.W., R. N. P.C., S.S., M. M. and J. D. A-C. All authors discussed the results and commented on the manuscript.

#### Funding

This work was financially supported by grants EP/J010413 and EP/J010391 for Aston University and the University of Plymouth from the UK Engineering and Physical Sciences Research Council. To access the data underlying this publication, please contact researchdata@aston.ac.uk. S.S. and M.M. thank the Ministry of Education, University and Research (MIUR) for financial support through the scientific program SIR2014 Scientific Independence of young Researchers (RBSI1455LK).

#### Declaration of interests

None



## References

- Aghamiri, Z.S., Mohsennia, M., Rafiee-Pour, H.A., 2018. *Talanta* 176, 195–207.
- Alexander, B., Browne, D.J., Reading, S.J., Benjamin, I.S., 1999. *J. Pharmacol. Toxicol.* 41, 55–58.
- Allsop, T., Neal, R., Mou, C., Brown, P., Saied, S., Rehman, S., Kalli, K., Webb, D.J., Sullivan, J., Mapps, D., Bennion, I., 2009. *Appl. Opt.* 48 (2), 276–286.
- Allsop, T., Neal, R., Mou, C., Kalli, K., Saied, S., Rehman, S., Webb, D.J., Culverhouse, P.F., Sullivan, J.L., Bennion, I., 2012. *J. Quantum Electron.* 48 (3), 394–405.
- Allsop, T., Mou, C., Neal, R., Mariani, S., Nagel, D., Tombelli, S., Poole, A., Kalli, K., Hine, A., Webb, D.J., Culverhouse, P., Mascini, M., Minunni, M., Bennion, I., 2017. *Opt. Express* 25 (1), 39–58.
- Ash, M., Ash, I., 1995. *Handbook of Plastic and Rubber Additives*, Gower Hampshire, UK.
- Attie, A.D., Raines, R.T., 1995. *J. Chem. Educ.* 72 (2), 119–123.
- Bennion, I., Williams, J.A.R., Zhang, L., Sugden, K., Doran, N.J., 1996. *Opt. Quant. Electron* 28 (2), 93–135.
- Boltz, U., Hagenmaier, H., Korner, W., 2001. *Environ. Pollut.* 115, 291–301.
- Brockman, J.M., Nelson, B., Corn, R., 2000. *Annu. Rev. Phys. Chem.* 51, 41–63.
- Ermini, M.L., Mariani, S., Scarano, S., Minunni, M., 2013. *Biosens. Bioelectron.* 40 (1), 193–199.
- Fromme, H., Kuchler, T., Otto, T., Pilz, K., Wenzel, A., 2002. *Water Res.* 36, 1429–1438.
- Furhacker, M., Scharf, S., Weber, H., 2000. *Chemosphere* 41 (5), 751–756.
- Hayat, A., Marty, J.L., 2014. *Front. Chem.* 2, 41.
- Heemken, O.P., Reincke, H., Stachel, B., Theobald, N., 2001. *Chemosphere* 45, 245–259.
- Homola, J., 2008. *Chem. Rev.* 108, 462–493.
- Huo, X., Chen, D., He, Y., Zhu, W., Zhou, W., Zhang, J., 2015. *Int. J. Environ. Res. Public Health* 12 (9), 11101–11116.
- Jo, M., Ahn, Ji-Y., Lee, J., Lee, S., Hong, S.W., Yoo, J.W., Kang, J., Dua, J.P., Lee, D.K., Hong, S., Kim, S., 2011. *Oligonucleotides* 21 (2), 85–91.
- Lee, B., Roh, S., Park, J., 2009. *Opt. Fiber Technol.* 15, 209–221.
- Liu, L.L., Marques, L., Correia, R., Morgan, S.P., Lee, S.W., Tighe, P., Fairclough, L., Korposh, S., 2018. *Sens. Actuators B: Chem.* 271, 24–32.
- Ma, Y., Liu, J., Li, H., 2017. *Biosens. Bioelectron.* 92, 21–25.
- Marks, H.L., Pishko, M.V., Jackson, G.W., Cote, G.L., 2014. *Anal. Chem.* 86 (23), 11614–11619.
- Mei, Z., Qu, W., Deng, Y., Chu, H., Cao, J., Xue, F., Chen, W., 2013. *Biosens. Bioelectron.* 49, 457–461.
- Mirzajani, H., Cheng, C., Wu, J., Chen, J., Eda, S., Aghdam, E.N., Ghavifekr, H.B., 2017. *Biosens. Bioelectron.* 89, 1059–1067.
- Moriyama, K., Tagami, T., Akamizu, T., Usui, T., Saijo, M., Kanamoto, N., Hataya, Y., Shimatsu, A., Kuzuya, H., Nakao, K., 2002. *J. Clin. Endocrinol. Metab.* 87 (11), 5185–5190.
- Oppeneer, S.J., Robien, K., 2015. *Public Health Nutr.* 18 (10), 1847–1863.
- Patskovsky, S., Kabashin, A., Meunier, M., Luong, J., 2003. *J. Opt. Soc. Am. A* 20 (8), 1644–1650.
- Ragavan, K.V., Rastogi, N.K., Thakur, M.S., 2013. *TrAC Trends Anal. Chem.* 52, 248–260.
- Rodríguez-Mozaz, S., De Alda, M.L., Barceló, D., 2005. *Water Res.* 39 (20), 5071–5079.
- Santos, A., Bueno, P.R., Davis, J.J., 2018. *Biosens. Bioelectron.* 100, 519–525.
- Segner, H., Carroll, K., Fenske, M., Janssen, C.R., Maack, G., Pascoe, D., Schaefer, C., Vandenberg, G.F., Watts, M., Wenzel, A., 2003. *Ecotoxicol. Environ. Saf.* 54, 302–314.
- Spoto, G., Minunni, M., 2012. *J. Phys. Chem. Lett.* 3 (18), 2682–2691.
- Toppari, J., Larsen, J.C., Christiansen, P., Giwercman, A., Grandjean, P., Guillelte, L.J., Skakkebaek, N.E., 1996. *Environ. Health Perspect.* 104 (Suppl 4), 741–803.
- Vandenberg, L.N., Hauser, R., Marcus, M., Olea, N., Welshons, W.V., 2007. *Reprod. Toxicol.* 24, 139–177.
- Watabe, Y., Kondo, T., Morita, M., Tanaka, N., Haginaka, J., Hosoya, K., 2004. *J. Chromatogr. A* 1032 (1–2), 45–49.
- Xiao, H., Edwards, T.E., Ferré-D’Amaré, A.R., 2008. *Chem. Biol.* 15 (10), 1125–1137.
- Yesilkoy, F., Terborg, R.A., Pello, J., Belushkin, A.A., Jahani, Y., Pruner, V., Altug, H., 2018. *Light: Sci. Appl.* 7 (2), 17152.
- Zheng, X., Li, L., Cui, K., Zhang, Y., Zhang, L., Ge, S., Yu, J., 2018. *ACS Appl. Mater. Interfaces* 10 (4), 3333–3340.